ISIJ International, Vol. 46 (2006), No. 8, pp. 1218–1222

Initial Stage of Localized Corrosion in Artificial Pits Formed with Photon Rupture on 55mass%Al–Zn Coated Steels

Masatoshi SAKAIRI, Yoshiyuki UCHIDA and Hideaki TAKAHASHI

Graduate School of Engineering, Hokkaido University, Kita-13, Nishi-8, Kita-ku, Sapporo 060-8628 Japan.

(*Received on February 23, 2006; accepted on May 19, 2006*)

The photon rupture method, whose oxide film and metal are removed by focused pulsed Nd–YAG laser beam irradiation was applied to form artificial micro pits in 55 mass% aluminum–zinc coated steels. The 15 μm coated layer was removed by 2 s of continuous laser irradiation in this experiment. The rest potential transients were measured during the laser irradiation. While the coated layer covered the steel substrate, the rest potential change in the negative direction just after the starts of the laser irradiation and then returned to the previous value. However, after the steel substrate was exposed to solution, the rest potential moved in the positive direction immediately after the discontinuation of the laser irradiation and then also returned to the previous value. The amplitude and duration of the potential changes after the laser irradiation increased with longer irradiation, related to the pit depth and exposed area ratio of coated layer/steel substrate. These rest potential fluctuation differences can be explained by galvanic reaction changes in the artificial pit formed on the coated steel during irradiation.

KEY WORDS: 55mass%Al–Zn coated steel; artificial pit; localized corrosion; chloride ions; photon rupture method.

1. Introduction

Zinc and its alloy coated steels are widely used because of their excellent corrosion protection characteristics in atmospheric environments. The corrosion protection of the coated layers are ascribed to cathodic protection by a galvanic reaction between the coated layer and substrate,[1–3] and the formation of stable and compact corrosion products which have high corrosion resistance. The composition of corrosion products formed on steels caused by atmospheric corrosion has been investigated in a range of exposure conditions.[4–8]

To examine abruptly destroyed passive oxide films and their repair are important to help understand the localized corrosion of metals. Analysis of this behavior has been carried out by monitoring potential- and current-transients after mechanical stripping of oxide films.[9–13] The mechanical film stripping poses problems in the film stripping rate, contamination from stripping tools, and stress and strain on the substrate.

Recently, there are reports of film stripping by a photon rupture method (focused pulses of pulsed YAG-laser irradiation), which resolves a lot of the problems caused by mechanical film stripping. The irradiation with a pulsed laser beam is able to strip oxide film at extremely high rates without contamination from the film removing tools. This technique has been applied to iron by Oltra *et al.*[14] and by Itagaki *et al.*,[15] and to aluminum electrodes,[16] and to zinc and its aluminum alloy coated steel by Sakairi *et al.*[17–25] This technique has also been applied to form micro patterns on metals,[26,27] and Sakairi *et al.* has reported on the effect of zinc and steel area ratios in artificial pits, which were formed on coated steels by photon rupture, on the rest potential change direction.[28] After laser irradiation, the rest potential changes in the negative direction while the zinc coated layer is exposed to the solution,. However, after the steel substrate is also exposed to the solution, the rest potential changes in the positive direction.

The purpose of this study is to investigate the effect of the area ratio of the coated layer and steel substrate of artificial pits in 55mass%Al–Zn coated steels by subject to photon rupture, on the initial stage of localized dissolution in 0.5 kmol m^{-3} H_3BO_3–0.05 kmol m^{-3} $Na_2B_4O_7$ (pH 7.4) with 0.01 kmol m^{-3} NaCl solutions.

2. Experimental

2.1. Specimen

The 55mass%Al–Zn coated steel sheets (coated layer thickness of about 15 μm, Nippon Steel Co.) were cut into 15×20 mm coupons. After cleaning ultrasonically, samples were dipped in a nitrocellulose/ethyl acetate solution two times to form an approximately 30 μm thick protective nitrocellulose film on the samples.

2.2. Electrochemical Measurements

Polarization curves of the coated layer and steel substrate, coated layer was chemically and mechanically removed, were measured by a potential scanning method, 0.3 mV/s in 0.5 kmol m^{-3} H_3BO_3–0.05 kmol m^{-3} $Na_2B_4O_7$ (pH 7.4) with 0.01 kmol m^{-3} NaCl solutions.

After formation of the nitrocellulose film, the specimens

were immersed in 0.5 kmol m^{-3} H_3BO_3–0.05 kmol m^{-3} $Na_2B_4O_7$ (pH 7.4) with 0.01 kmol m^{-3} NaCl solutions, and irradiated by a pulsed Nd–YAG laser (Sepctra Physics GCR-130) through a lens and quartz window at open circuit condition. The laser beam was the second harmonic wave, wave length 532 nm, wave duration 8 ns, and frequency 10 s^{-1}, the laser power was adjusted to 30 mW before the lens. The irradiation interval was 0.1 s. The rest potential transients of the specimens after the laser irradiation were measured by a computer through an A/D converter. The laser irradiation time was also detected by a photo-detector.

A saturated Ag/AgCl electrode was used as a reference electrode to measure the electrochemical data.

2.3. Surface Observation

After the tests, the specimen surfaces were examined by a con-focal scanning laser microscope (CSLM, Laser Tech. Co.). The artificial pit depth was measured by the depth analysis function of the CSLM.

3. Results

3.1. Polarization Behavior

Figure 1 shows polarization curves of 55mass%Al–Zn coated steel and steel substrate in 0.5 kmol m^{-3} H_3BO_3–0.05 kmol m^{-3} $Na_2B_4O_7$ (pH 7.4) with 0.01 kmol m^{-3} NaCl solutions. The rest potential of the 55mass%Al–Zn coated layer is about −1 V and it is almost the same as Zn and Zn–5mass%Al coated steels. The anodic current of the coated layer increases with increasing potential at low over potentials, decreases with the potential, and then increases with potentials higher than about −0.8 V. During cathodic polarization, the current decreases with decreasing potential. The anodic current of the steel substrate increases with increasing potential at low over potentials, decreases with the potential, and then increases with potentials higher than about 0 V. Between −0.4 V and 0 V, the current changes with current fluctuation, which may be related to birth and death process of localized corrosions. During cathodic polarization, the current decreases with decreasing potential.

3.2. Formation of the Artificial Pits

The CSLM contrast images after different periods, t_i=0.1 and 10 s, of laser irradiation are shown in **Fig. 2**. Both the coated layer, the central dark area, and the nitrocellulose film are removed by one pulse, t_i=0.1 s, of laser irradiation. The shape is almost circular and the diameter of the coated layer removed is about 130 μm with the area of nitrocellulose film removed about 300 μm. The shape and the size of the removed area at t_i=0.1 s are almost the same as those at t_i=10 s. This figure indicated that the depth of the removed area of the 55mass%Al–Zn coated layer becomes deeper with irradiation time. The result suggests that it is possible to make artificial micro-pits, which shape is almost cylindrical, on coated steel and also to change the area ratio between steel and aluminum–zinc alloy by this technique. The aspect-ratio of artificial pits is less than 0.4. The exposed area of coated layer was calculated that the outer rim of the irradiated area and wall of the pit which shape is almost cylindrical. The exposed area of steel was calculated that the shape is almost cylindrical. The area ratio of steel substrate/coated layers exposed to solution change from 0 to about 0.3 in these experiments.

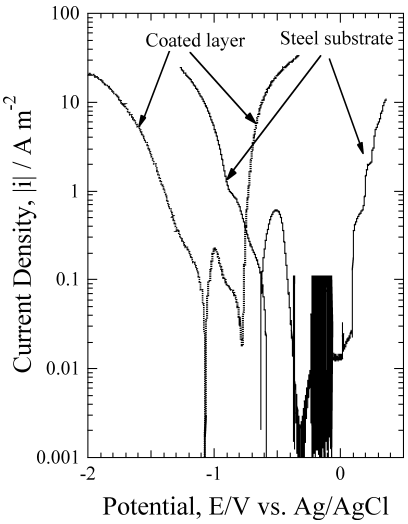

Fig. 1. Polarization curves of 55mass%Al–Zn coated steel and steel substrate in 0.5 kmol m^{-3} H_3BO_3–0.05 kmol m^{-3} $Na_2B_4O_7$ (pH 7.4) with 0.01 kmol m^{-3} NaCl solutions. Sweep rate: 0.33 mV/s.

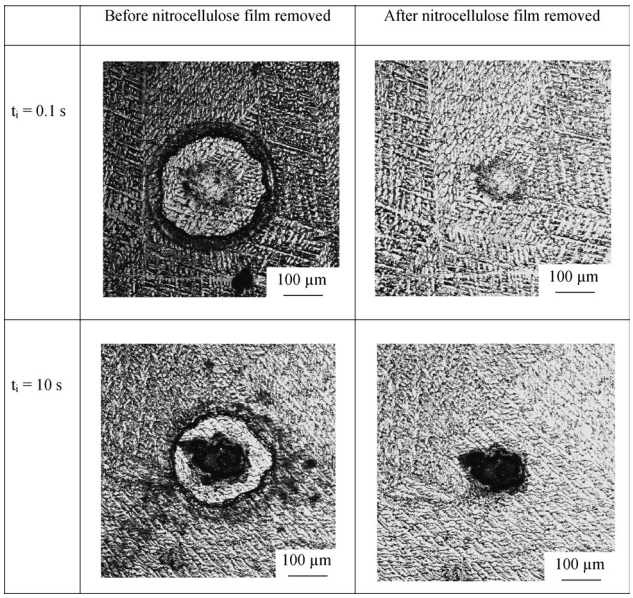

Fig. 2. CSLM contrast images after different periods, t_i=0.1 and 10 s, of laser irradiation.

Figure 3 shows the changes in the pit depth with irradiation duration in 0.5 kmol m^{-3} H_3BO_3–0.05 kmol m^{-3} $Na_2B_4O_7$ solutions. The pits become deeper with irradiation time and the depth is almost the same as the Al–Zn coated layer thickness after about 2 s of continuous irradiation. The slope also changes after the coated layer is removed at the irradiated area because of removal efficiency differences between the coated layer and steel, which depends on the reflectivity and thermal properties of the materials. These results show that about 2 s is enough to remove the coated layer. Hence, only the coated layer is exposed to the solution at stage I, and both zinc and steel substrate are exposed to the solution at stage III. Parts of the substrate are exposed to the solution at stage II, the interval between stages

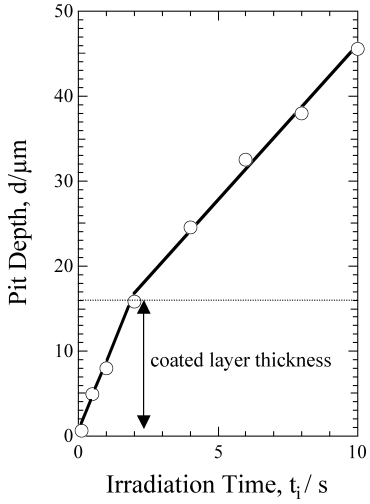

Fig. 3. Changes in the artificial pit depth with irradiation time in 0.5 kmol m^{-3} H_3BO_3–0.05 kmol m^{-3} $Na_2B_4O_7$ with 0.01 kmol m^{-3} NaCl solutions.

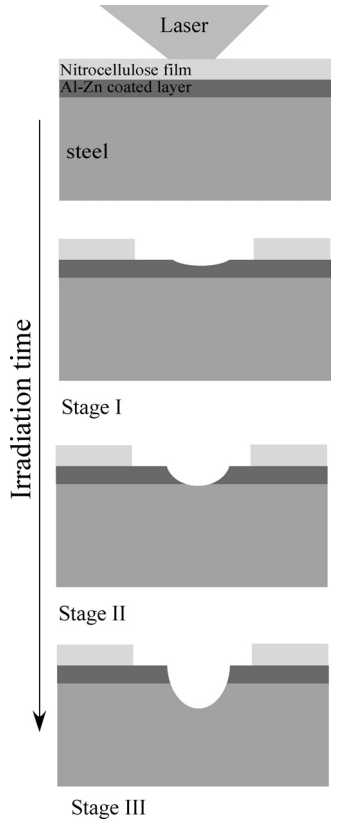

Fig. 4. Schematic outline of cross sections of each stage of laser irradiation.

I and II. **Figure 4** is a schematic outline of cross sections at each stage. The area ratio of steel substrate/coated layers exposed to solution was 0 at stage I, it was about 0.2 at stage II, and it was changed from about 0.2 to about 0.3 with irradiation period at stage III.

3.3. Rest Potential Changes after Laser Irradiation

Figure 5 shows changes in the rest potential with time during continuous laser irradiation in 0.5 kmol m^{-3} H_3BO_3–0.05 kmol m^{-3} $Na_2B_4O_7$ with 0.01 kmol m^{-3} NaCl solutions. Before laser irradiation, the rest potential showed positive values because the specimen surface was covered by nitrocellulose film. The rest potential suddenly moving in the negative direction after one pulse of laser irradiation, this potential is lower than immersion potential of the specimen in Fig. 1. The rest potential may be reflected in the standard electrode potential of aluminum and zinc, because of bear surface of coated layer may exposed to the solution after one pulse of laser irradiation. During continuing laser irradiation, the rest potential moves in the positive direction with potential fluctuations, at a frequency similar to the pulse frequency of the laser. The potential after 10 s of laser irradiation reaches the almost same potential as rest potential of the steel substrate. This may be related mixed potential of cathodic reaction on steel substrate and anodic dissolution of coated layer.

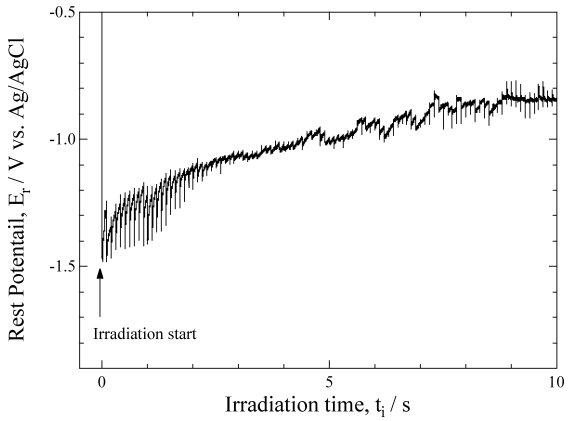

Fig. 5. Changes in the rest potential with time during continuous laser irradiation in 0.5 kmol m^{-3} H_3BO_3–0.05 kmol m^{-3} $Na_2B_4O_7$ with 0.01 kmol m^{-3} NaCl solutions.

Figure 6 shows typical example of changes in the rest potential with time after laser irradiation at stage I, stage II and stage III in Fig. 5. The rest potential suddenly decreases after the laser irradiation and shows a peak and then returns to previous value at stage I. However, the rest potential shift direction at stage III is opposite to that at stage I. The rest potential direction of the shift changes during stage II, because stage II is a transitional stage between stage I and stage III.

4. Discussion

4.1. Formation Speed of Pits

The approximate expression for the minimum laser power density of ablation, E_{av}, is $2 \cdot L \cdot r \cdot k^{0.5} \cdot t_p^{-0.5}$, where t_p is the pulse duration, L is the latent heat required to vaporize the solid metal, k is the thermal diffusibility and r is the density of the metal.[29] From this equation, the laser power density have about 10^{12} W/m^2 is above the E_{av} of both the coated layer and steel substrate. The adsorbed power density, E_{ad}, is expressed by $E_{ad}=4(1-R)P/(\pi \cdot D^2 \cdot t_p)$, where P is the irradiated laser power density, D is the diameter of the irradiated area, and t_p is the pulse duration. The adsorbed power density can be estimated to be about 4×10^{12} W/m^2 in these experiments. Altogether, this indicates that the artificial pit was formed by laser ablation forming gas or plasma. The latent heat for vaporization of the coated

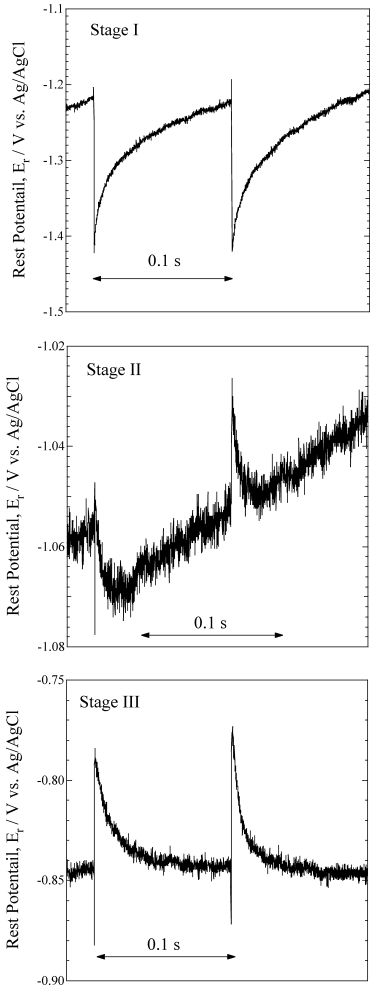

Fig. 6. Typical example of changes in the rest potential with time after laser irradiation at stage I, stage II and stage III in Fig. 5.

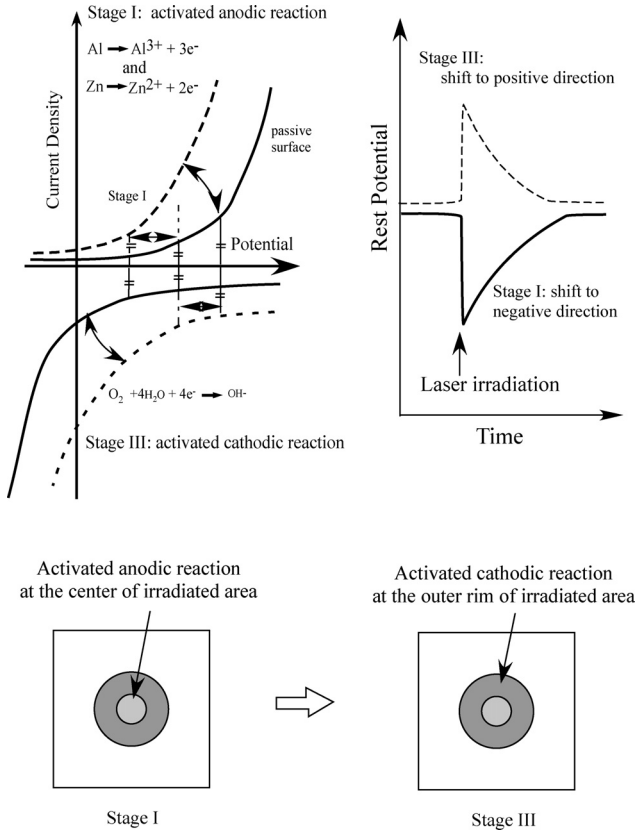

Fig. 7. Schematic outline of polarization curve changes, rest potential changes and activation site changes with time at stages I and III.

layer is half that of the steel substrate. If the adsorbed laser power was similar at every stage, the formation speed of the artificial pit in the steel substrate is slower than that of coated layer.

4.2. Potential Fluctuations

Figure 7 shows a schematic outline of the anodic and cathodic polarization curves, before (solid line) and after (dotted line) laser irradiation, with a schematic drawing of current changes. In this study, the anodic and cathodic reactions are as below and the cathodic reaction site would change during the continuous laser irradiation.

$$\left.\begin{aligned} &Zn \rightarrow Zn^{2+} + 2e^- \\ &Al \rightarrow Al^{3+} + 3e^- \end{aligned}\right\} \quad \text{Anodic reactions}$$

$$O_2 + 2H_2O + 4e^- \rightarrow 4OH^- \quad \text{Cathodic reaction}$$

And the activation site in this study at every stage is center of irradiated area which size is about 130 μm in diameter.

At stage I, the anodic reaction site is the center of the irradiated area where the coated layer has been removed and the cathodic reaction site is the outer rim of the irradiated area where the coated layer has not yet been removed by the continuous laser irradiation. During the laser irradiation, the anodic reaction, metal dissolution, may be activated because oxide film or corrosion product is removed at the anodic reaction site. This means the anodic polarization curve changes after the laser irradiation. If there is no change in the cathodic reaction at stage I, the rest potential would change in the negative direction. After some period, the activated area may be covered by corrosion products or oxide film, this would cause the rest potential to return to its previous value. The area of both reactions should be exchange at stage III. Because of this area change, the cathodic reaction on steel substrate is activated by the laser irradiation at stage III, and the rest potential changes in the positive direction after the start of laser irradiation. After some period, the activated area may be covered by corrosion products or oxide film, causing the rest potential to return to the previous value.

5. Conclusions

The effect of the area ratio of the coated layer and steel substrate in artificial pits, formed in 55mass%Al–Zn coated steels by photon rupture, on the initial stage of localized dissolution was examined, and the following conclusions may be drawn.

(1) An artificial micro pit can be formed in a coated layer by continuous focused pulsed YAG laser irradiation. The pit diameter remains constant and the depth increases with increasing time of irradiation. The pits formation speed in the coated layer is higher than that in the steel substrate.

(2) After laser irradiation, the rest potential changes in

the negative direction while the zinc coated layer is exposed to the solution. However, after the steel substrate is also exposed to the solution, the rest potential changes in the positive direction. These differences in rest potential changes in direction can be explained by changes in the activated reactions by laser irradiation.

Acknowledgements

The authors are indebted to The Iron and Steel Institute of Japan for financial support and thank Nippon Steel Co. for providing the coated steel sheets.

REFERENCES

1) G. X. Zhang: Corrosion and Electrochemistry of Zinc, Plenum Publication, New York, (1996), 183.
2) Y. Hisamatsu: *Bull. Jpn. Inst. Met.*, **20** (1981), 3.
3) Y. Miyoshi, J. Oka and S. Maeda: *Trans. Iron Steel Inst. Met.*, **23** (1983), 974.
4) T. E. Graedel: *J. Electrochem. Soc.*, **136** (1989), 193C.
5) J. E. Svensson and L. G. Johansson: *J. Electrochem. Soc.*, **143** (1996), 51.
6) J. E. Svensson and L. G. Johansson: *Corros. Sci.*, **34** (1993), 721.
7) J. J. Frei: *Corrosion*, **42** (1986), 422.
8) S. Oesch and M. Faller: *Corros. Sci.*, **39** (1997), 1505.
9) F. P. Ford, G. T. Burstein and T. P. Hoar: *J. Electrochem. Soc.*, **127** (1980), 1325.
10) G. T. Burstein and P. I. Marshall: *Corros. Sci.*, **23** (1983), 125.
11) G. T. Burstein and R. C. Newman: *Corros. Sci.*, **21** (1981), 119.
12) G. T. Burstein and R. J. Cinderey: *Corros. Sci.*, **32** (1991), 1195.
13) R. J. Cindery and G. T. Burnstein: *Corros. Sci.*, **33** (1992), 493.
14) R. Oltra, G. M. Indrianjafy and R. Roberge: *J. Electrochem. Soc.*, **140** (1993), 343.
15) M. Itagaki, R. Oltra, B. Vuillemin, M. Keddam and H. Takenouti: *J. Electrochem. Soc.*, **144** (1997), 64.
16) M. Sakairi, Y. Ohira and H. Takahashi: *Electrochem. Soc. Proc.*, **97-26** (1997), 643.
17) M. Sakairi, K. Itabashi and H. Takahashi: *Corros. Sci. Technol.*, **31** (2002), 426.
18) M. Sakairi, K. Itabashi and H. Takahashi: Proc. of Japan-China Joint Seminar on Marin Corrosion, Tokyo Inst. Tech., Tokyo, (2002), 58.
19) M. Sakairi, K. Itabashi and H. Takahashi: *Electrochem. Soc. Proc.*, **2002-24** (2002), 399.
20) M. Sakairi, K. Itabashi and H. Takahashi: Proc. of Int. Symposium Corrosion Science in the 21st Century, UMIST, Manchester, (2003), C093.
21) M. Sakairi, K. Itabashi and H. Takahashi: *Zaiyro-to-Kankyo*, **52** (2003), 524.
22) M. Sakairi, K. Itabashi and H. Takahashi: Proc. of 13th APCCC, APCCC 13, Japan Society of Corrosion Engineering, Tokyo, (2003), 62.
23) M. Sakairi, K. Itabashi and H. Takahashi: *ISIJ Int.*, **45** (2005), 71.
24) M. Sakairi, K. Itabashi, Y. Uchida and H. Takahashi: *Corros. Sci.*, **47** (2005), 2461.
25) M. Sakairi, K. Itabashi, Y. Uchida and H. Takahashi: *Tetsu-to-Hagané*, **92** (2006), 16.
26) T. Kikuchi, M. Sakairi and H. Takahashi: *J. Electrochem. Soc.*, **150**, (2003), C567.
27) T. Kikuchi, M. Sakairi, H. Takahashi, Y. Abe and N. Katayama: *Surf. Coat. Technol.*, **169** (2003), 199.
28) M. Sakairi, Y. Uchida and H. Takahashi: Proc. of Passivity 9, Elsevier B.V., London, in press.
29) C. B. Scruby and L. El Drain: Laser Ultrasonics—Techniques and Applications, Adam Hilger, New York, (1990), 243.